



Investigation of a copper–nickel alloy resistor using co-electrodeposition

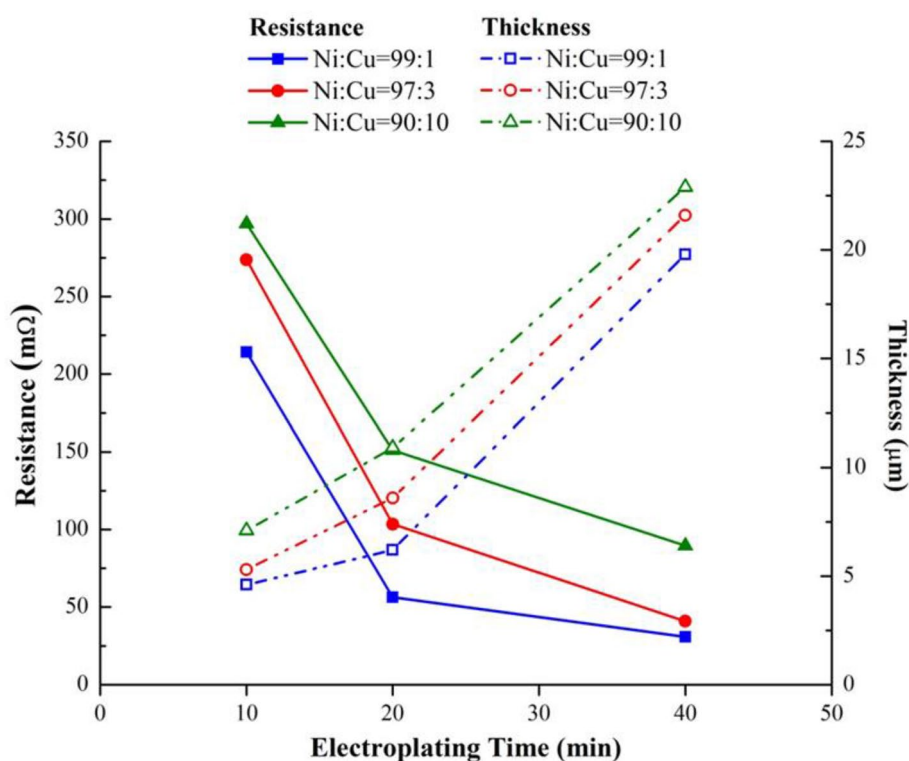
Wen-His Lee¹ · K. C. Chung¹

Received: 22 April 2019 / Accepted: 1 November 2019 / Published online: 9 March 2020
© Springer Nature B.V. 2020

Abstract

Using this co-electrodeposition method, we successfully prepared a Cu–Ni alloy film at a low temperature. The results of this study showed that when Cu–Ni film is co-deposited at -1.3 V (vs. Ag/AgCl) in a solution with a composition ratio of Ni to Cu ions of 90:10, the atomic percentage of Cu to Ni necessary to form the Cu–Ni alloy is approximately one. Electroplated for 20 min, the thickness of the Cu–Ni film grows to around $10\ \mu\text{m}$, and the resistance is approximately $103\ \text{m}\Omega$. In this work, the samples were annealed at 700, 800, and $900\ ^\circ\text{C}$ for 30 min, respectively. The resistance increased gradually with increases in the annealing temperature because of the increasing entropy of the Cu–Ni alloy. On the contrary, the TCR decreased gradually with increases in the annealing temperature. The sample annealed at $900\ ^\circ\text{C}$ exhibited a single crystal FCC Cu–Ni alloy with a lattice constant of $3.62\ \text{\AA}$, corresponding to a very low TCR of around $50\ \text{ppm}/^\circ\text{C}$.

Graphic Abstract



Thickness and resistance as a function of plating time at -1.3 V (vs. Ag/AgCl)

Keywords Co-electrodeposition · Cu–Ni alloy · TCR

Extended author information available on the last page of the article

1 Introduction

Copper–nickel alloys (Cu–Ni alloys), which were previously called cupronickel have gained a variety of interesting applications owing to their specific characteristics [1]. As super alloys, Cu–Ni alloys have excellent corrosion ability [2, 3] and are applied widely in marine engineering. In addition, they are used in nuclear power engineering [4]. Cu–Ni alloys with specific compositions contribute to different properties as well as different applications. Since most pure metals have a positive temperature coefficient of resistance (TCR) of several thousand ppm/ °C, Cu–Ni alloy with a 45 atomic percent of Ni, known as a “constantan,” provides low resistivity and a low TCR. This ensures low, constant electric resistance over a wide range of temperatures and has recently been applied in thin film configurations for resistive components [5, 6].

The traditional Cu–Ni alloy fabrication process is very expensive since it requires an extremely high temperature to make the Cu and Ni melt into the liquid phase, after which Cu atoms and Ni atoms flow randomly. Therefore, the objective of this study is to fabricate Cu–Ni alloys at a relatively low temperature. The electrodeposition process has a high deposition rate as is inexpensive, so it is promising as an alternative method to fabricate Cu–Ni alloys [7].

When Cu and Ni are mixed for co-deposition, Cu deposition becomes relatively dominant because Cu has a higher reduction potential than Ni. The quantitative and qualitative behavior of the co-electrodeposition of Ni and Cu based on their mixing solution differs significantly from that of the individual single-metal solution. Some studies have found that the composition ratio of the alloy deposition can be mutually controlled by (1) the bath compositions, (2) the pH/temperature, (3) the applied potential/current densities, (4) the growth mechanism, and (5) the displacement reaction.

In this study, we used 20 μm of a sintered aluminum paste as the experimental substrate. Then, we co-deposited Cu and Ni film in the solutions containing different composition ratios of Cu to Ni at a constant voltage. The standard reduction reactions for reductions of Ni and Cu are -0.23 V and $+0.34$ V, respectively. We expected to obtain a film with a specific atomic ratio of Cu to Ni. Lastly, we would further apply a heat treatment that altered the physical and chemical properties of the samples. After annealing, Cu atoms and Ni atoms migrated randomly in the crystal lattices to form the Cu–Ni alloy phase. Using this method, the cost to fabricate alloys can be reduced.

2 Experimental procedure

Figure 1a shows a schematic diagram depicting the three parts of this study: (1) the preparation of Al paste on an Al_2O_3 substrate, (2) Cu–Ni co-electrodeposition and annealing, and (3) a materials analysis and measurement of electric properties.

The flow for preparing the Al-thick film paste specimens on the Al_2O_3 substrate is shown in Fig. 1b. Screen printing was used to print the Al paste onto the Al_2O_3 substrates, after which they were placed in an oven for drying at 200 °C for 15 min. and then sintered at 850 °C for 60 min in a box furnace.

The electrolytic solution containing $\text{CuSO}_4\cdot 5\text{H}_2\text{O}(\text{s})$ for Cu ions, $\text{NiSO}_4\cdot 6\text{H}_2\text{O}(\text{s})$ for Ni ions, and $\text{C}_6\text{H}_5\text{Na}_3\text{O}_7\cdot 2\text{H}_2\text{O}(\text{s})$ (sodium citrate) as complexing agents for co-electroplating were prepared as shown in Fig. 1c. Nickel solution was composed by nickel aminosulfonate ($\text{Ni}(\text{NH}_2\text{SO}_3)_2\cdot 4\text{H}_2\text{O}$), nickel chloride ($\text{NiCl}_2\cdot 6\text{H}_2\text{O}$) and boric acid (H_3BO_3) and Copper solution was composed by copper sulfate ($\text{CuSO}_4\cdot 5\text{H}_2\text{O}$), sulfuric acid (H_2SO_4), chloride (Cl^-). The total saturated metal ion concentration was maintained at 0.38 M while the citrate concentration was 0.31 M.

Tripolar plating system was used in this experiment, the reference electrodes are Calomel electrode and Ag/AgCl electrode relative to S. H. E is 0.197 V, the auxiliary electrode is a thin slice of 99.99% pure platinum electrode with the dimensions of 1×4 cm², and the working electrode is Al electrode coated on the Al_2O_3 substrate. A plating solution was also used to conduct cyclic voltammetry (Potentiostat/Galvanostat PGSTAT302 N produced by Metrohm Autolab B.V.). As shown in Table 1, electrolyte compositions of Cu/Ni ratio for co-electroplating was varied from 99/01, 97/03 to 90/10 pH was kept at 1.5 and the scanning range was from 0 to -1.5 V at 5 mVs⁻¹.

We co-electroplated Cu and Ni onto the specimens in the electrolytic solution with different molar ratios of Ni to Cu ions. All the electroplating experiments were performed at solution temperature of 50 °C. The co-electrodeposition specimens were placed sequentially in the tube furnace for annealing in an atmosphere of inert gas and N_2 at different temperatures. The electrical properties, such as the resistance and temperature coefficient of resistance, of the Ni–Cu co-electrodeposition samples after annealing were measured with a four-point probe from JANDEL RM3000. A microstructure examination and phase identification of the Cu–Ni co-electrodeposition specimens before/after annealing were analyzed using XRD, SEM, and TEM, respectively.

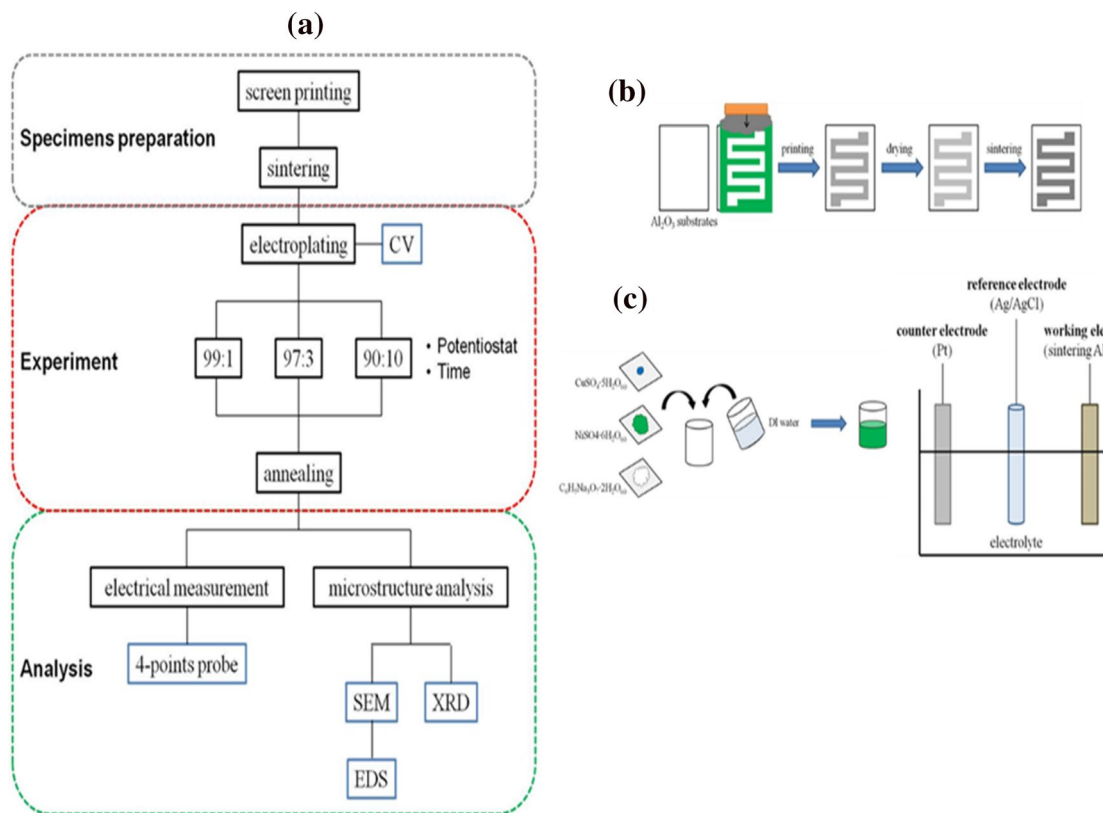


Fig. 1 Schematic diagram of the experiment procedures

Table 1 Electrolyte compositions for co-electroplating

Ni: Cu (molar ratio)	99:1 (g)	97:3 (g)	90:10 (g)
$\text{CuSO}_4 \cdot 5\text{H}_2\text{O}_{(s)}$	0.476	1.426	4.760
$\text{NiSO}_4 \cdot 6\text{H}_2\text{O}_{(s)}$	49.470	48.470	44.970
$\text{C}_6\text{H}_5\text{Na}_3\text{O}_7 \cdot 2\text{H}_2\text{O}_{(s)}$	45.520	45.520	45.520

3 Results and discussion

3.1 Cyclic voltammetry

The scan rate of the cyclic voltammograms with different proportions of NiSO_4 and CuSiO_4 varied from 99/01, 97/03 and 90/10 at 5 mV/s from the positive potential (0 V) to the negative potential (−1.5 V). As shown in Fig. 2, the forward scan produced a current peak for the species in solution that could be reduced or oxidized depending on the initial scan direction through the range of the potential scanned. The current increases as the potential reaches the reduction potential of the species in solution but then falls off as the concentration of the species in solution is depleted close to the surface of the working electrode. According to these curves, they can basically be divided

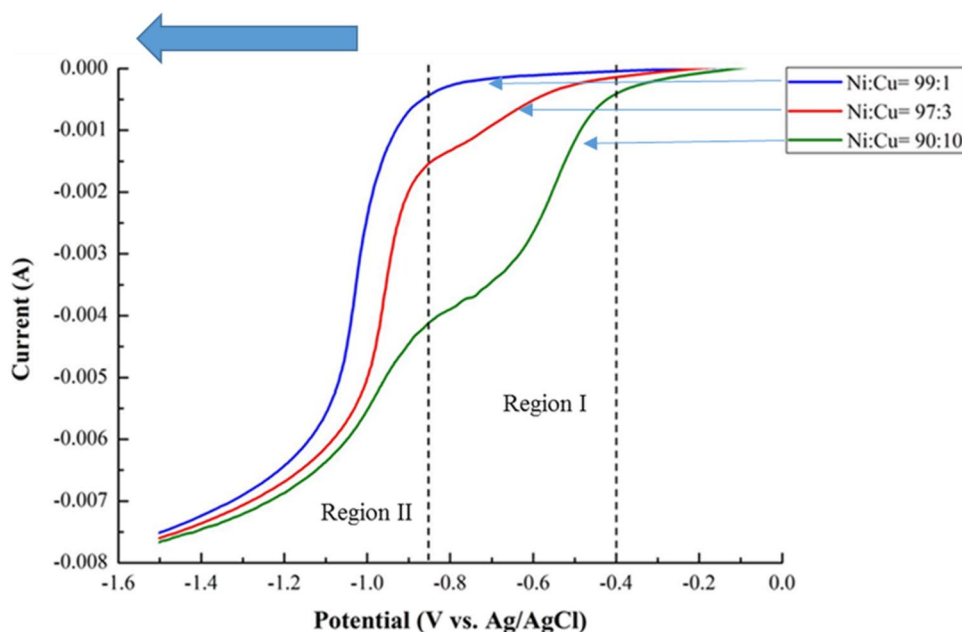
into two regions. In the potential region between −0.40 and −0.85 (vs. Ag/AgCl), called region (I), there appeared to be a current increase with more Cu content in the different electrolytes. This means that the copper–citrate complex in the solution obtained electrons, which could be attributed to the formation of the deposited Cu layer. Ni electrodeposition is controlled by charge transfer, while Cu electrodeposition is controlled by the diffusion of Cu ions [8]. In addition, there seems to be the start of another electrode reaction at −0.85 V (vs. Ag/AgCl), the reduction of Ni. The curves achieve the limiting current at −1.30 V (vs. Ag/AgCl), and this limitation is mainly related to the mass transport of nickel ions [9]. The potential between −0.80 and −1.30 V (vs. Ag/AgCl) is proposed for our studies.

3.2 Analysis of Cu–Ni co-electrodeposition film at −0.9 V (vs Ag/AgCl)

To co-electroplate Cu–Ni alloys on the surface of the specimens simultaneously, we set the electrode potential constant at −0.9 V and −1.3 V (vs. Ag/AgCl), which, according to CV curves shown in Fig. 2, were more negative than the reduction potential of Cu (+0.34 V) and Ni (−0.23 V).

Since the electrochemical reaction at the working electrode is very complicated, as mentioned earlier, since the

Fig. 2 Cyclic voltammograms from 0 to -1.5 V for the different electrolyte



reduction of hydrogen ions from the dissociation of hydrogenated citrate ion, oxygen reduction, Cu deposition, Ni deposition, and reduction of water lead to differences in the appearance of Cu–Ni in electrolytic solutions with various molar ratios. That is, the concurrent electrodeposition of Cu and Ni are not independent; a displacement reaction occurs between deposited nickel metal and copper ion in solution. This implies that the color of specimens electroplated in the electrolyte with more Cu content becomes darker, as shown in Fig. 3. The color is a matted silver, dark yellowish-green, or reddish brown, as shown in Fig. 3a–c.

The atomic percentage of the deposited coatings was determined using energy-dispersive spectroscopy (EDS). The results are shown in Fig. 4. We observed that with more Cu content in the electrolyte, there were more Cu atoms deposited on the surface of the specimens under potentiostatic conditions. In addition, according to the results, the atomic percent of Cu to Ni close to 1:1, which is known as a “constantan,” occurred when the specimen electroplated in the electrolyte had a molar ratio of Ni to Cu of 97:3.

In this study, secondary electron (SE) images using a scanning electron microscope (SEM) were obtained to reveal the surface microstructure morphology. As can be seen in Fig. 5, when more Cu atoms were deposited, there were more small clusters growing on the surface, and the shape of microstructure was more like cauliflower.

Figure 6 shows a comparison of the XRD patterns of Cu–Ni in the electrolyte with various ratios of Ni to Cu. It can be observed that there were peaks of Cu and Ni for the specimens in the electrolytic solution with ratios of Ni to Cu of 99:1 and 97:3, respectively. In addition, it can be seen that the peaks of Ni shifted slightly to the peaks of Cu because of more Cu content in the deposited film. However, there were only Cu peaks in the electrolyte solution with a ratio of Cu to Ni of 90:10 because the atomic proportion of Ni to Cu in the deposited layers was 8.66 to 91:34, in contrast to the other results shown in Fig. 4.

Fig. 3 Appearance of Cu–Ni in the different electrolyte at -0.9 V (vs. Ag/AgCl). 180 min, molar ratio is **a** Ni:Cu = 99:1, **b** Ni:Cu = 97:3, **c** Ni:Cu = 90:10

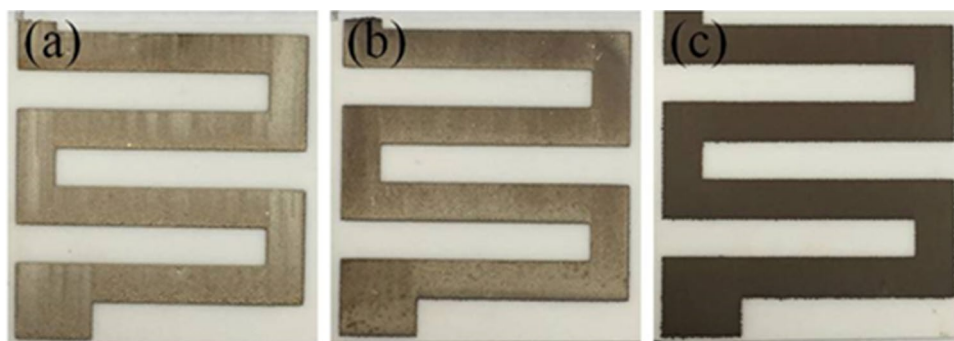


Fig. 4 Atomic percent of Cu–Ni in the different electrolyte at -0.9 V (vs. Ag/AgCl). 180 min, molar ratio is **a** Ni:Cu=99:1, **b** Ni:Cu=97:3, **c** Ni:Cu=90:10

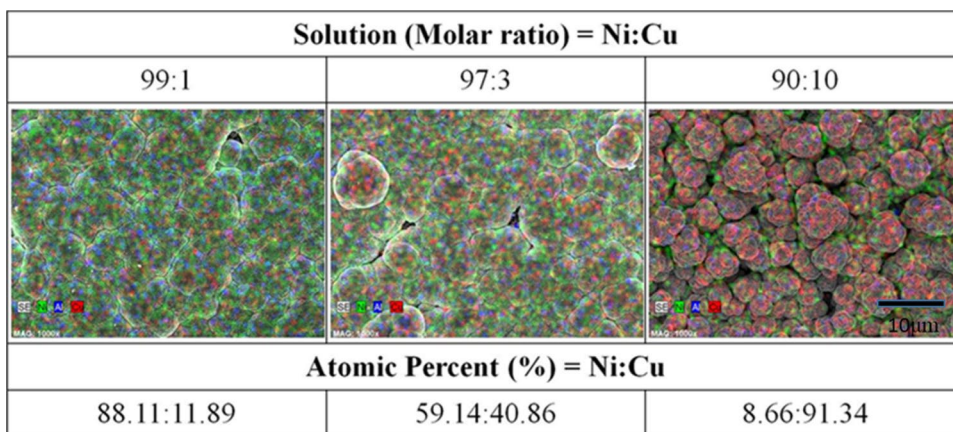


Fig. 5 Microstructure of Cu–Ni in the different electrolyte at -0.9 V (vs. Ag/AgCl). 180 min, molar ratio is **a** Ni:Cu=99:1, **b** Ni:Cu=97:3, **c** Ni:Cu=90:10

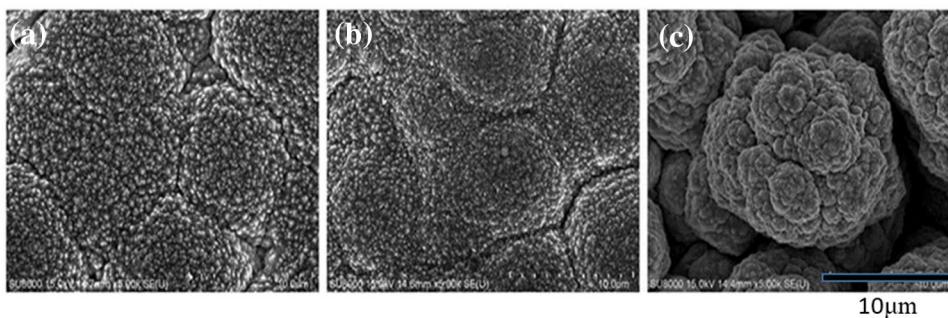
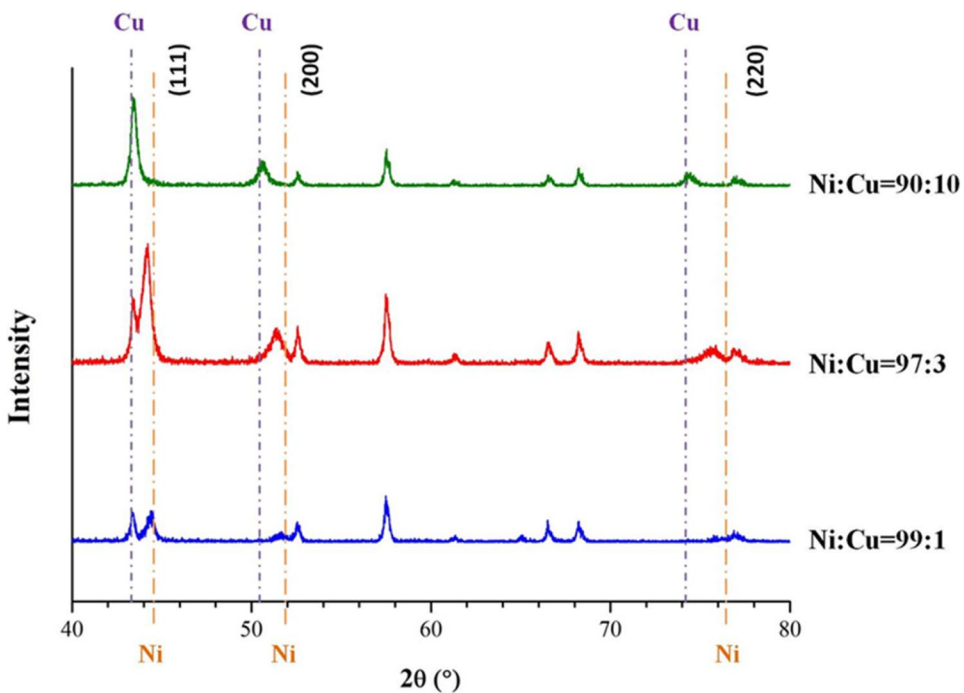


Fig. 6 XRD pattern of Cu–Ni in the different electrolyte at -0.9 V (vs. Ag/AgCl)



3.3 Analysis of co-electrodeposition of Cu–Ni film at -1.3 V (vs. Ag/AgCl)

It took approximately 3 h to co-deposit CuNi film with a thickness of $10\ \mu\text{m}$ at -0.9 V (vs. Ag/AgCl). Hence, to shorten the co-deposition time, we applied the output potential constant at -1.3 V (vs. Ag/AgCl).

The color of the specimens with less Ni content electroplated in the electrolyte became darker, as shown in Fig. 7. The color gradually became a dark yellowish-green from the silver, as shown in Fig. 7a–c. Compared with the appearance of the specimens shown in Fig. 3a, b, the corresponding colors in Fig. 7a, b are much brighter. However, the color in Fig. 7c can be clearly distinguished from that in Fig. 3c.

The atomic percentage of the deposit in the electrolyte with various molar ratios is shown in Fig. 8. It was

determined that the atomic percentage of Cu to Ni close to one was the specimen electroplated in the electrolyte with a molar ratio of Ni to Cu of 90:10. The results were different from those found at -0.9 V (vs. Ag/AgCl), as shown in Fig. 8.

Owing to a higher electrode potential, the corresponding current passing the circuit increased to 45–50 mA. As mentioned above, the current may affect the growth mechanism of the deposited layer, which leads to the crystal growing to a larger spherical cluster of grains, as shown in Fig. 9 compared with those shown in Fig. 5. While more Cu atoms deposited on the substrates, there were also lots of small spherical grains on the top surface, more like pop-corn.

Figure 10 provides a comparison of the XRD pattern of the Cu–Ni in the electrolyte with various ratios of Cu to Ni. It can be clearly observed that there were peaks of Cu and

Fig. 7 Appearance of Cu–Ni in the different electrolyte at -1.3 V (vs. Ag/AgCl). 20 min, molar ratio is **a** Ni:Cu=99:1, **b** Ni:Cu=97:3, **c** Ni:Cu=90:10

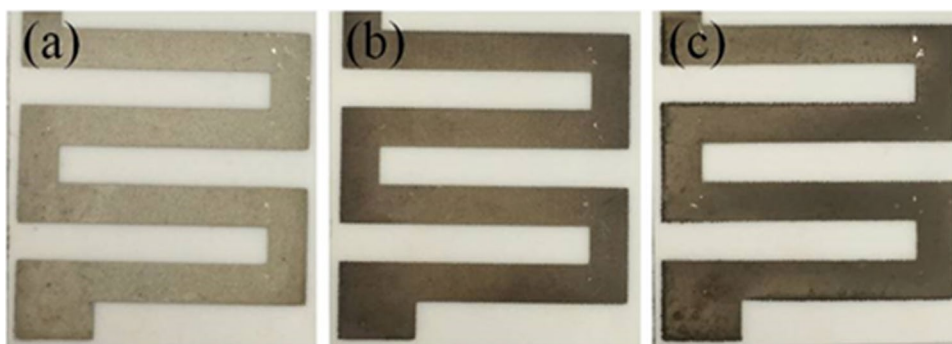
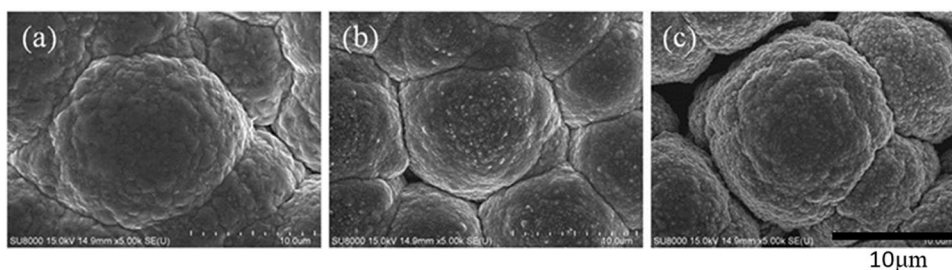


Fig. 8 Atomic percent of Cu–Ni in the different electrolyte at -1.3 V (vs. Ag/AgCl). 20 min, molar ratio is **a** Ni:Cu=99:1, **b** Ni:Cu=97:3, **c** Ni:Cu=90:10

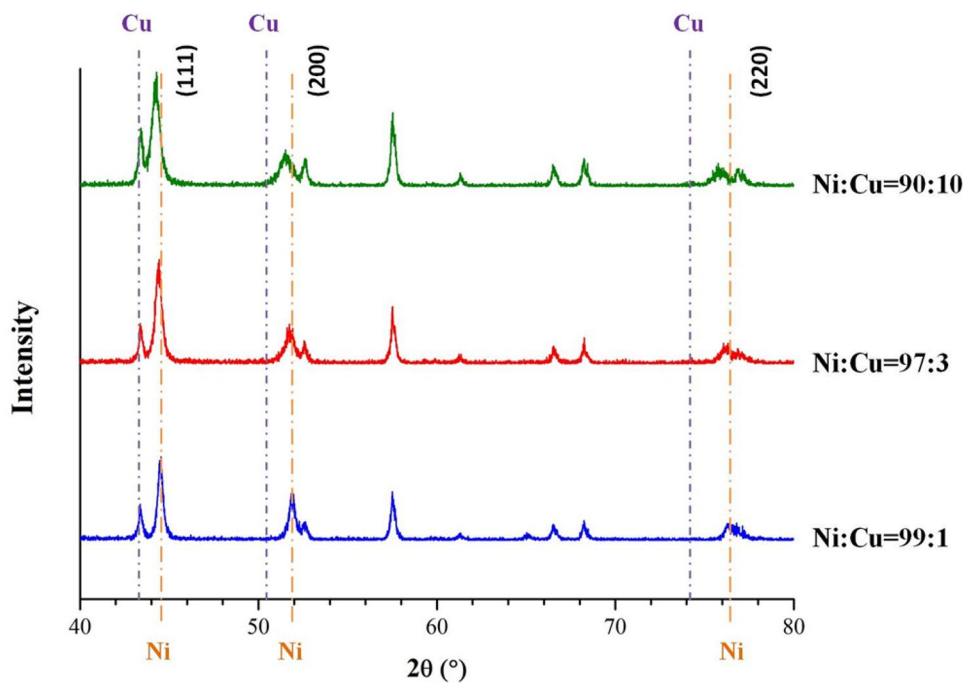
Solution (Molar ratio) = Ni:Cu		
99:1	97:3	90:10
Atomic Percent (%) = Ni:Cu		
97.50:2.50	82.23:17.77	61.37:38.63

Fig. 9 Microstructure of Cu–Ni in the different electrolyte at -1.3 V (vs. Ag/AgCl). 20 min, molar ratio is **a** Ni:Cu=99:1, **b** Ni:Cu=97:3, **c** Ni:Cu=90:10



10µm

Fig. 10 XRD pattern of Cu–Ni in the different electrolyte at -1.3 V (vs. Ag/AgCl)



Ni in the Cu to Ni electrolytic solution. In addition, it can also be seen the peaks of Ni slightly shifted to the Cu peaks with more Cu content in the electrolytic solution. This was because the atomic percentages of Ni to Cu for the deposited layer were different, as shown in Fig. 6. A comprehensive comparison of the two XRD results in the electrolytic solution with a ratio of Cu to Ni of 90:10 at -0.9 V (vs. Ag/AgCl) and at -1.3 V (vs. Ag/AgCl) shows that there were only peaks of Cu when electroplating at -0.9 V (vs. Ag/AgCl), but there were peaks of both Cu and Ni when electroplating at -1.3 V (vs. Ag/AgCl).

3.4 Measurement of resistance and thickness for the co-electrodeposited Cu–i film

Figure 11 shows that the surface coverage of the deposited layer became denser with increases in the electroplating time and increases in the ratio of Cu to Ni in the electrolytic solution. This result was associated with the higher deposition rate of Cu as compared to Ni.

Figure 12 shows a cross-section of specimens co-electroplated at the constant -1.3 V (vs. Ag/AgCl). It can be clearly seen that a uniform, continuous co-deposited Cu–Ni film was obtained and that the thickness of the deposited film increased with increases in the plating time. The top layer of the Cu–Ni film used as the resistive layer obtained by co-plating is denser than that of the bottom layer of the Al film as the seed layer obtained from thick film firing.

Figure 13 shows the relationship between thickness and resistance as function of co-deposition time, where it can be seen that the thickness of the film linearly increased with

increases in the co-depositing time for three kinds of electrolytes with different ratios of Ni to Cu. It took 10 min to deposit a layer of around 5 μm . Each deposited layer grew over 20 μm during 40 min of electroplating. However, the thickness of film is increased with increases in the proportion of Cu in the electrolyte at -1.3 V (vs. Ag/AgCl) with the same co-depositing time. This result was attributed to the high deposition rate of Cu in the electrolyte.

As shown in Fig. 13, the thickness of co-deposited film at -1.3 V (vs. Ag/AgCl) for 20 min in the electrolyte with ratios of Ni to Cu of 99:1, 97:3, and 90:10 were 7 μm , 9 μm and 11 μm , respectively. Deposition rates of Ni/Cu at concentration ratio of 99/01, 97/03, 90/10 at -1.3 V are 0.53 , 0.58 , 0.66 $\mu\text{m}/\text{min}$. In addition, it was found that the resistance of co-deposited film at -1.3 V (vs. Ag/AgCl) for 20 min in the electrolyte with ratios of Ni to Cu of 99:1, 97:3, and 90:10 was 56 $\text{m}\Omega$, 103 $\text{m}\Omega$, and 151 $\text{m}\Omega$, respectively. It is worth noting that the thicker co-deposited film in the electrolyte with different ratios of Ni to Cu exhibited higher resistance in terms of the co-deposited film. Theoretically, resistance is inversely proportional to thickness of film [10]. However, Fig. 13 shows the relationship between film thickness and resistance, where it appears that the difference in resistance was not only due to the thickness of film but was also due to other factors.

The formula for sheet resistance is shown as follows:

$$R_s = \rho/t,$$

where R_s is the sheet resistance; ρ is the resistivity, and t is thickness.

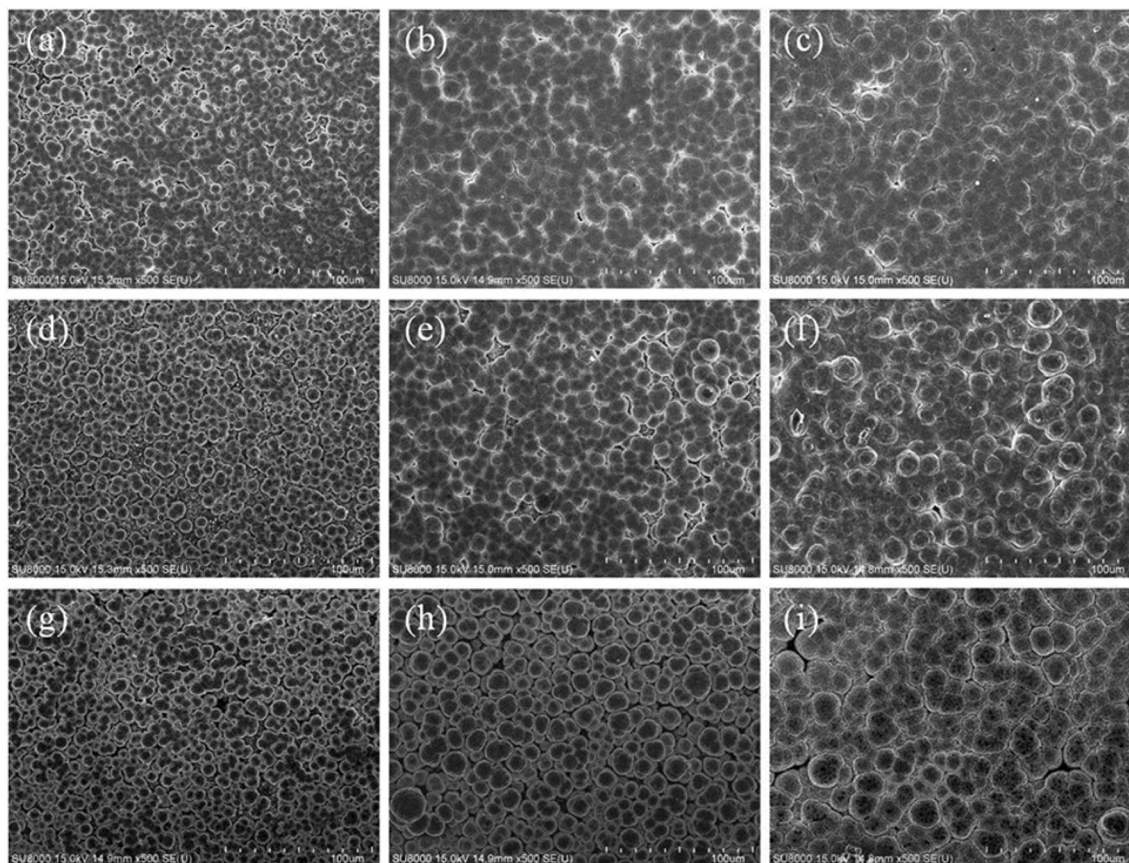


Fig. 11 SEM top view images of Cu–Ni under various experiment conditions at -1.3 V Ni:Cu=99:1, **a** 10 min, **b** 20 min, **c** 40 min, Ni:Cu=97:3, **d** 10 min, **e** 20 min, **f** 40 min, Ni:Cu=90:10, **g** 10 min, **h** 20 min, **i** 40 min

Based on the above formula, the resistivity of the co-deposited film at -1.3 V (vs. Ag/AgCl) for 20 min in the electrolyte with ratios of Ni to Cu of 99:1, 97:3 and 90:10 was 3.92×10^{-7} m Ω , 9.27×10^{-7} m Ω and 16.61×10^{-7} m Ω , respectively. Thus, an electrolyte with a high ratio of Ni to Cu exhibits high resistivity in the co-deposited film. The total resistivity is the sum of the contributions from thermal vibrations, impurities, and plastic deformation. Therefore, the proportion of the atomic percent of Cu to Ni in the film is a key to determining the resistivity of materials and the resistance of film. The resistivity was shown to reach a maximum when the ratio of two components in the alloy is close to one [11]. Thus, the resistivity increased with increases in the proportion of the atomic percent of Cu in the CuNi alloy before reaching a ratio close to one. The composition of the co-deposited alloy film at -1.3 V (vs. Ag/AgCl) for 20 min in the electrolyte with the ratio of Ni to Cu of 99:1, 97:3 and 90:10 was 98:2, 82:18, and 61:39. Obviously, the resistivity of the co-deposited Cu–Ni alloy film increased with increases in the molar ratio of Cu to Ni in the Cu–Ni alloy.

3.5 Effect of annealing on phase formation and crystallization

To obtain Cu–Ni alloys with a low TCR, two parameters were chosen that could make the Cu to Ni ratio of the deposited layer close to 1 as well as the same thickness for the purposes of an annealing treatment, the first of which was the specimen in the electrolyte with a ratio of Ni to Cu of 90:10 electroplated for 20 min at -1.3 V (vs. Ag/AgCl).

To obtain complete Cu–Ni alloys with a low-TCR characteristic, we chose the specimen in the electrolyte with a ratio of Ni to Cu of 90:10 electroplated for 20 min at -1.3 V (vs. Ag/AgCl) to make the Cu to Ni of the deposited layer close to 1 using high-temperature annealing in an N₂ atmosphere.

Figure 14 provides photographs of the specimens prepared after annealing. The specimen was annealed for 30 min at 700 °C, 800 °C, and 900 °C from the left to the right, respectively. Comparing the results shown in Fig. 14 with the corresponding specimen before annealing shown in Fig. 7, it can be clearly observed that the color turns

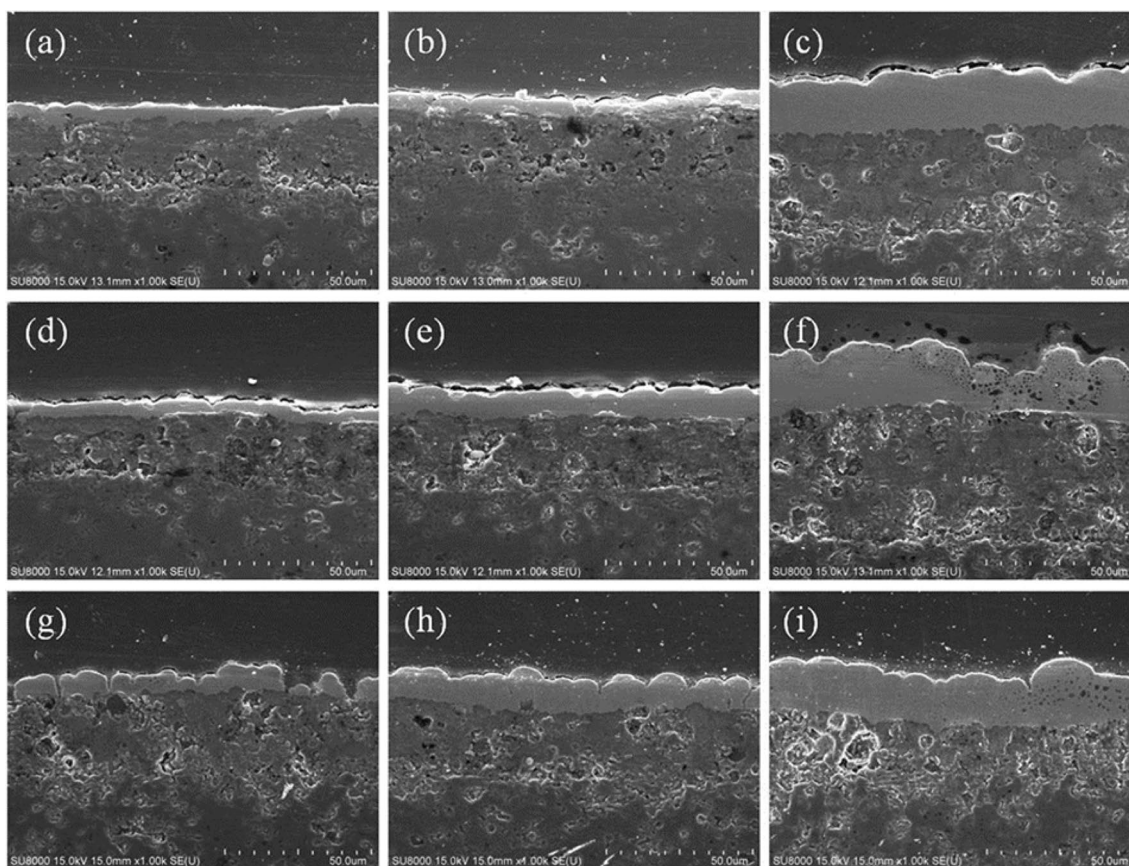


Fig. 12 SEM cross-section images of Cu–Ni under various experiment conditions at -1.3 V Ni:Cu=99:1, **a**, 10 min **b** 20 min, **c** 40 min, Ni:Cu=97:3, **d** 10 min, **e** 20 min, **f** 40 min, Ni:Cu=90:10, **g** 10 min, **h** 20 min, **i** 40 min

from khaki into silver after annealing at a high temperature. Figure 15 shows the top view of the SEM images of the specimen in the electrolyte with a ratio of Ni to Cu of 90:10 electroplated for 20 min at -1.3 V (vs. Ag/AgCl) after annealing. It can be observed that the grains in the cluster of the deposited layer become larger and smoother with increases in the annealing temperature. This is probably because the grains pass through recovery, recrystallization, and grain growth behavior while heating up to the critical temperature and then cooling in the furnace to form ordered alloys, which is a change in the crystal orientation. This treatment can also restore the mechanical properties of a material.

Figure 16 shows a cross-section of the SEM images and EDS mapping results for the specimen in the electrolyte with a ratio of Ni to Cu of 90:10 electroplated for 20 min at -1.3 V (vs. Ag/AgCl) after annealing at 700, 800, and 900 °C, respectively. Based on the SEM images, it was determined that the Ni atoms and Cu atoms randomly distributed in the deposited layer.

Figure 17 shows a series of XRD patterns of the specimen in the electrolyte with a ratio of Ni to Cu of 90:10 electroplated for 3 h at -1.3 V (vs. Ag/AgCl) after annealing at different temperatures. The XRD peaks of $\text{Cu}_{50}\text{Ni}_{50}$ in the JCPD database were used for comparison to determine at which annealing temperature the ordered alloys were formed. It was found that the patterns of the specimens after annealing, as shown in Fig. 17, were close to the standard peaks of $\text{Cu}_{50}\text{Ni}_{50}$ at all of the annealing temperatures and that the crystalline structure of the Cu–Ni alloy was enhanced with increases in the annealing temperature [12].

Figure 18, 19 provides a microstructure examination of the specimen in the electrolyte with a ratio of Ni to Cu of 90:10 electroplated for 20 min at -1.3 V (vs. Ag/AgCl) after annealing at 900 °C using TEM. Clearly, Fig. 18 shows perfect crystallization after annealing. Figure 19 is the selected area electron diffraction (SAED) pattern corresponding to Fig. 18. It shows that the specimen in the electrolyte with a ratio of Ni to Cu of 90:10 electroplated for 20 min at -1.3 V (vs. Ag/AgCl) after annealing at 900 °C is a single phase of

Fig. 13 Thickness and resistance as a function of plating time at -1.3 V (vs. Ag/AgCl)

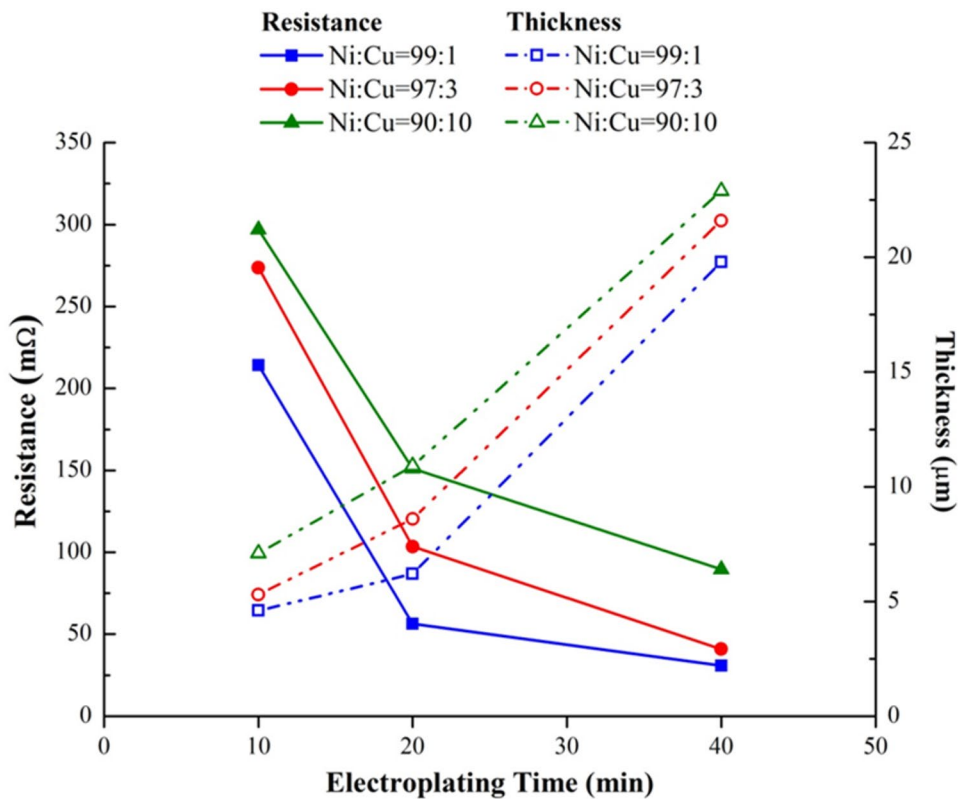


Fig. 14 Appearance of Cu–Ni at -1.3 V (vs. Ag/AgCl) after annealing. **a** 700 °C, **b** 800 °C and **c** 900 °C

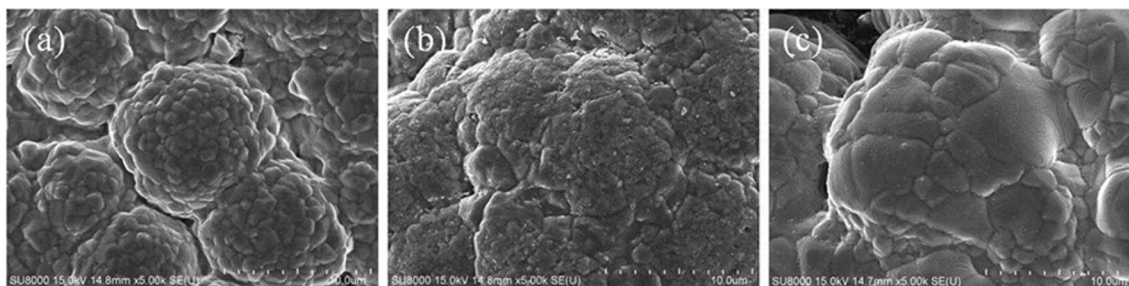
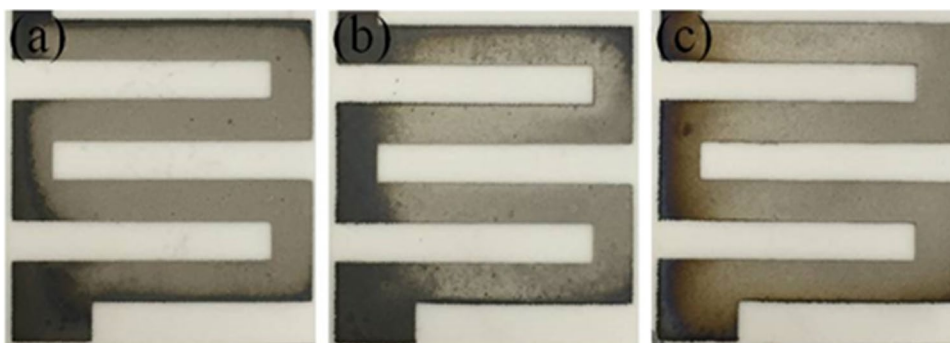


Fig. 15 SEM images of microstructure at -1.3 V (vs. Ag/AgCl) after annealing. **a** 700 °C, **b** 800 °C and **c** 900 °C

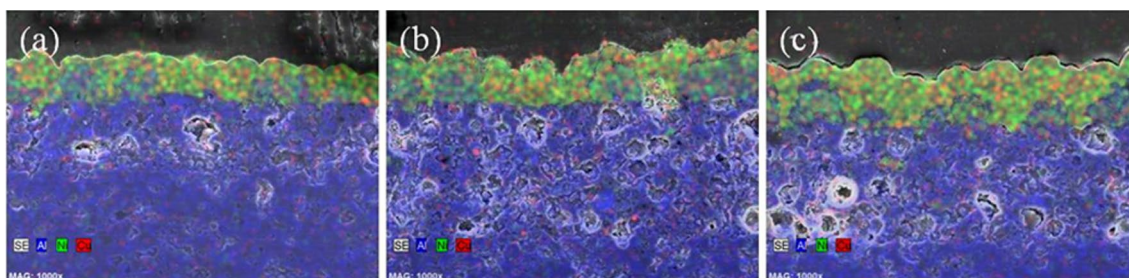
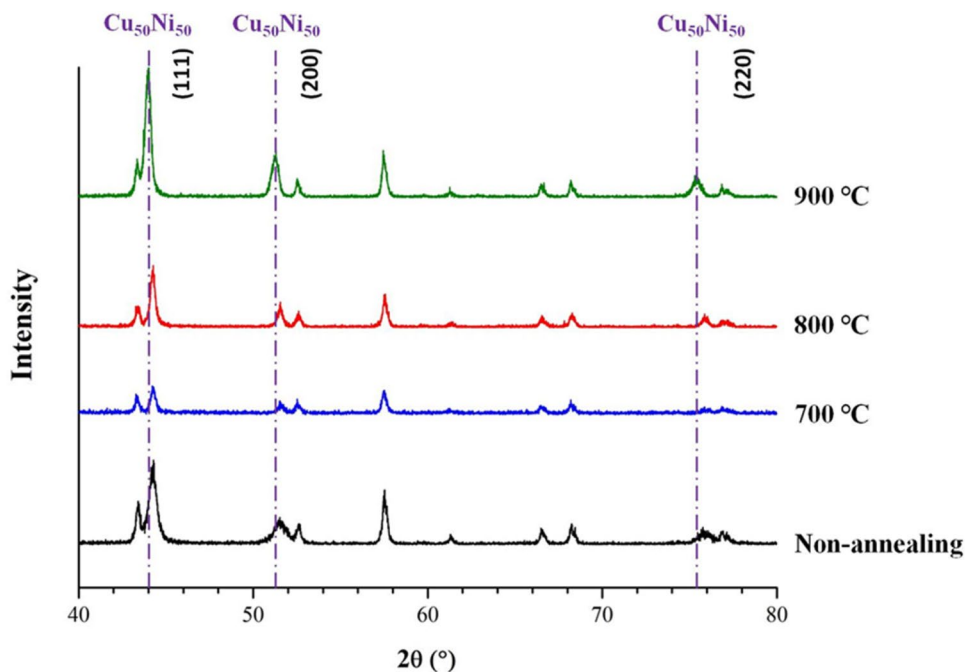


Fig. 16 SEM images of cross-section at -1.3 V (vs. Ag/AgCl) after annealing. **a** 700 °C, **b** 800 °C and **c** 900 °C

Fig. 17 A series of XRD pattern at -1.3 V (vs. Ag/AgCl) after annealing



the Cu–Ni alloy. Each spot corresponds to the diffraction condition of the crystal structure. We measured the distance between a selected spot and a fixed spot using a scale bar (d-spacing). One was 1.81 Å, and the other was 1.11 Å. These two d-spacing measurements separately corresponded to the crystal plane (200) and (311) results in the lattice constant 3.62 Å, the FCC structure of the Cu–Ni alloy [13].

3.6 Measurement of electrical properties for co-electrodeposited and annealed Cu–Ni alloy film

The temperature coefficient of resistant (TCR) can be calculated from the formula shown below:

$$\text{TCR (ppm/}^{\circ}\text{C)} = \left[\frac{(R_{155} - R_{25})}{R_{25}} \right] / ((155 - 25)) \times 10^{-6},$$

where R_{155} is the resistance measured at 155 °C, and R_{25} is the resistance measured at 25 °C, which is room temperature.

Figure 20 shows the relationship between the resistance and TCR of the specimen in the electrolyte with a ratio of Ni to Cu of 90:10 electroplated for 20 min at -1.3 V (vs. Ag/AgCl) for different annealing temperature. We observe that the resistance increased gradually with increases in the annealing temperature because of the increasing entropy of the Cu–Ni alloy. On the contrary, the TCR decreased gradually with increases in the annealing temperature as a result of a formation of Cu–Ni alloys phase, as mentioned in previous studies [14]. The Cu atoms and Ni atoms in the deposited layer rearranged to form a strong bond with each other through high temperature annealing. In addition, it was found that the TCR of the specimen in the electrolyte with a ratio of Ni to Cu of 90:10 electroplated for 20 min at -1.3 V (vs. Ag/

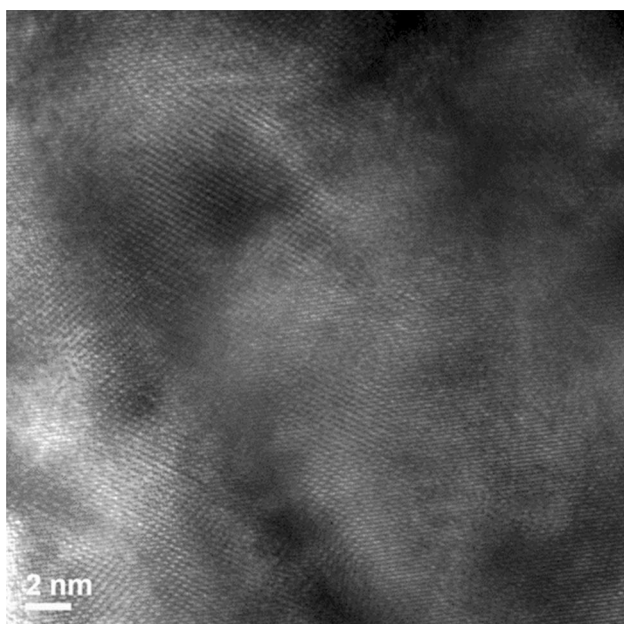


Fig. 18 TEM image of Cu–Ni at -1.3 V (vs. Ag/AgCl) after annealing at 900 °C

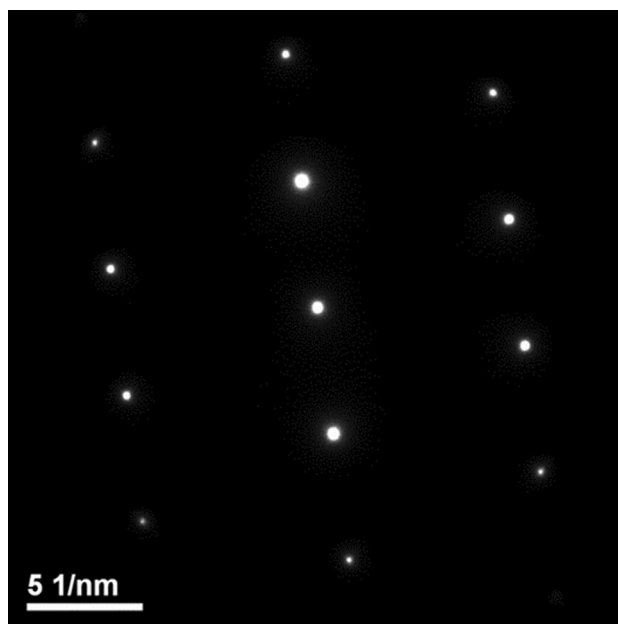


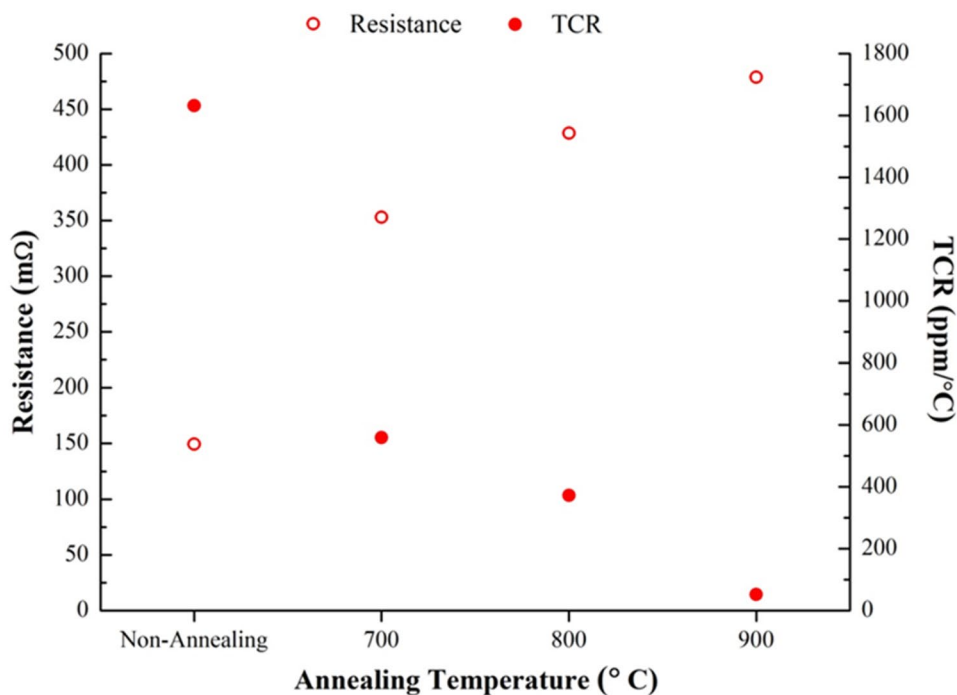
Fig. 19 SAED pattern of Cu–Ni at -1.3 V (vs. Ag/AgCl) after annealing at 900 °C

AgCl) after annealing at 900 °C was around 50 ppm/°C. There may have been electron scattering due to dislocation and other crystal defects, as well as from the grain boundaries. All of these scattering processes add to the resistivity of a metal, just as in the scattering process resulting from impurities. We can, therefore, write the effective resistivity of a metal as.

$$\rho = \rho_T + \rho_I,$$

where ρ_I is due to the scattering of electrons by impurities, which is only slightly temperature-dependent [15]. In an isomorphous alloy of two metals, that is, a binary alloy of Cu–Ni that forms a solid solution, the temperature-independent impurity contribution ρ_I increases with the concentration

Fig. 20 Resistance and TCR as function of annealing temperature at -1.3 V (vs. Ag/AgCl)



of solute atoms. This means that as the Ni alloy concentration increases, the degree of disorder increases, and resistivity ρ increases and becomes less temperature-dependent as ρ_I overwhelms ρ_T [16].

4 Conclusion

1. In this study, we have successfully demonstrated that a high-crystalline Cu–Ni alloy reflecting very low TCR performance can be achieved by co-electrodeposition and annealing at a relatively low temperature of 900 °C for 30 min.
2. A electrodeposition of Cu–Ni alloy film with an atomic percent of Cu to Ni close to 1:1 and thickness of 9 μm exhibited a resistance of 103.5 m Ω and a TCR of 1631.9 ppm/°C was obtained. The crystallization of Cu–Ni alloys after co-electrodeposition at 50 °C is not good enough and further annealing is necessary.
3. With increases in the annealing temperature, the resistance of the sample with co-electrodeposition is gradually increased, but TCR of sample is gradually decreased. The samples annealed at 900 °C for 30 min exhibited very promising electrical properties, including a low TCR of 51.5 ppm/°C and a resistance of 478.7 m Ω , corresponding to a perfect single crystal of Cu–Ni alloy with an FCC structure and lattice constant of 3.62 Å, based on examination using XRD and TEM.

Acknowledgements This research received financial support from MOST of Taiwan. 107-2622-E-006-011-CC3.

Affiliations

Wen-His Lee¹ · K. C. Chung¹

✉ Wen-His Lee
leewen@mail.ncku.edu.tw

References

1. Grimshaw P, Calo JM, Hradi G (2011) *Ind Eng Chem Res* 50:9532–9538
2. Wu H, Wang Y, Zhong Q, Sheng M, Du H, Li Z (2011) *J Electroanal Chem* 663:59–66
3. Varea A, Pellicer E, Pané S, Nelson BJ, Suriñach S, Baró MD, Sort J (2012) *Int J Electrochem Sci* 7:1288–1302
4. Badawy WA, Ismail KM, Fathi AM (2005) *Electrochem Acta* 50:3603–3608
5. Subramanian V, Chandramohan P, Srinivasan MP, Velmurugan S, Narasimhan SV (2007) *Corros Sci* 49:620–636
6. Yusop NK, Shariff NM, Chow SC, Ismail AB (2016) *Procedia Chem* 19:619–625
7. Ying RY, Patrick K, Ng J (1988) *Electrochem Soc*
8. Callister WD, Rethwisch DG (2011) *Materials science and engineering*, 8th edn. Wiley, Asia, pp 406–416
9. Hearnea SJ, Floro JA (2005) Mechanisms inducing compressive stress during electrodeposition of Ni. *J Appl Phys* 97:014901
10. Lee JM, Lee SH, Kim YJ, Ko JS (2013) *Int J Precis Eng Manuf* 14:2009–2014
11. Ollivier A, Muhr L, Delbos S, Grand PP, Matlosz M, Chassaing E (2009) *J Appl Electrochem* 39(12):2337–2344
12. Serin N, Serin T, Horzum S, Çelik Y (2005) *Semicond Sci Technol* 20(5):398
13. Varea A, Pellicer E, Pané S et al (2012) *Int J Electrochem Sci* 7(2012):1288–1302
14. Hur SG, Kim DJ, Kang BD, Yoon SG (2005) *J Electrochem Soc* 152:G472–G476
15. Chang JK, Hsu SH, Sun IW, Tsai WT (2008) *J Phys Chem C* 112(5):1371–1376
16. Zhang Y, Zuo T, Cheng Y (2013) Liaw PK High-entropy alloys with high saturation magnetization, electrical resistivity, and malleability. *Sci Rep* 3:1455

Publisher's Note Springer Nature remains neutral with regard to jurisdictional claims in published maps and institutional affiliations.

¹ Department of Electric Engineering, National Cheng-Kung University, Tainan, Taiwan